Asian Journal of Chemistry; Vol. 37, No. 12 (2025), 3127-3135
ASIAN JOURNAL OF CHEMISTRY
https://doi.org/10.14233/ajchem.2025.34806

Design, Synthesis, Characterization and Molecular Docking Studies of Benzimidazole-2-thione, Benzoxazole-2-thione and Benzothiazole-2-thione Derivatives as Potential HSV and HIV Inhibitors

SOUKAINA ZAHM[1], SAID JEBBARI[2], ASSIYA ATIF[2,*], NABIL NOR[1], HATIM SOUFI[3], HOUSSINE AIT SIR[2], MOHAMED EL HOUSSE[4], HABIB EL ALAOUI EL ABDELLAOUI[1] and MOHAMMED SALAH[1]

[1]Molecular Modeling and Spectroscopy Research Team, Department of Chemistry, Faculty of Sciences, Chouaïb Doukkali University, El Jadida, Morocco
[2]Bioorganic Chemistry Team, Department of Chemistry, Faculty of Sciences, Chouaib Doukkali University, El Jadida, Morocco
[3]Laboratory of Applied Physical Chemistry of Materials, Department of Chemistry, Faculty of Sciences, Chouaib Doukkali University, El Jadida, Morocco
[4]Department of Applied Chemistry, Faculty of Sciences, Ibnou Zohr University, Agadir, Morocco

*Corresponding author: E-mail: assia.atif@gmail.com

Received: 31 August 2025 *Accepted*: 6 November 2025 *Published online*: 30 November 2025 AJC-22204

In this work, the synthesis of 16 novel compounds generated through condensation reactions employing *o*-phenylenediamine, *o*-aminophenol and *o*-aminothiol is carried out. The synthesized products comprised derivatives of benzimidazole-2-thione, benzoxazole-2-thione and benzothiazole-2-thione, obtained in yields ranging from 70% to 90%. Structural elucidation was performed using nuclear magnetic resonance spectroscopy, Fourier-transform infrared spectroscopy and high-resolution mass spectrometry. In addition, the study investigated the ADMET properties and dynamic molecular behaviour of the synthesized compounds. Significantly, this work introduces a novel synthetic strategy for generating derivatives of 2-mercapto-benzimidazole, 2-mercaptobenzoxazole and 2-mercaptobenzothiazole, providing valuable understanding of their chemical structures and underlying formation pathways. Furthermore, the inhibitor activity of these molecules against HIV and HSV viruses was assessed using a docking method as an alternative to traditional laboratory experiments, enhancing the efficiency of antiviral screening.

Keywords: Molecular docking studies, ADMET, Rhodamine, N-Aminopromazine, HSV inhibitor, HIV Inhibitor.

INTRODUCTION

The mercapto compounds have become increasingly important in recent years for the synthesis of a wide range of organosulfur compounds used in various fields, including organic synthesis, bioorganic chemistry, medicinal chemistry and heterocyclic chemistry [1-3]. Moreover, thiol groups act as reversible protecting groups in peptide synthesis, temporarily shielding reactive functionalities to prevent side reactions and allowing selective deprotection at later stages [4,5]. Overall, the use of mercapto compounds and thiol species has enabled the synthesis of a variety of new compounds and has provided valuable tools for organic and medicinal chemists.

Among the hybrid mercapto aromatic compounds, benzimidazole-2-thione, benzoxazole-2-thione and benzothiazole-2-thione are the sulfur-containing heterocycles in which a thione (C=S) group is positioned at the 2-site of a fused aromatic ring system. The presence of the thione moiety confers nucleophilic character, facilitating reactions with electrophilic species, while the heterocyclic nitrogen contributes to structural stability and modulates electronic properties. These compounds serve as key intermediates in the synthesis of diverse heterocycles and have broad applications in medicinal chemistry, agrochemical development and coordination chemistry. Their unique combination of reactivity and structural versatility makes them valuable scaffolds for constructing biologically active molecules and functional materials [6-8].

Benzothiazole and its derivatives have been extensively studied for their pharmacological potential, exhibiting a wide range of biological activities [9-12]. Several derivatives demonstrate anticancer effects, inhibiting the growth of breast, lung, prostate and colon cancer cells and showing promise in pre-

clinical models [12,13]. They also possess antimicrobial activity against pathogens such as methicillin-resistant *Staphylococcus aureus* (MRSA) and *Candida albicans* [14], antidiabetic effects through hypoglycemic activity [15], and antiviral properties, including inhibition of HSV and HIV replication [16-19]. These findings highlight the versatility of benzothiazole scaffolds in developing bioactive compounds.

Moreover, benzothiazole and its derivatives have shown promising preclinical activity, further studies are required to evaluate their safety and efficacy in humans. In this work, substituted benzimidazole-2-thioles are synthesized *via* the condensation of substituted *o*-phenylenediamines with N-aminorhodanine in the presence of catalysts such as triethylamine or acetic anhydride, proceeding through an imine intermediate that cyclizes to form the desired product [20-27]. This method allows incorporation of various substituents on the aromatic ring, yielding a diverse set of derivatives. Traditional syntheses using carbon disulfide (CS_2) or thiourea (CH_4N_2S) have also been reported [28-31], but CS_2 poses significant health hazards, including acute and chronic toxicity [32,33]. Thus, replacing CS_2 with N-aminorhodanine provides a safer and more eco-friendly approach, producing benzimidazole-2-thiole derivatives efficiently with good yields and structural diversity. Moreover, the inhibitory potential of the synthesized molecules against HIV and HSV was investigated using computational docking, complemented by ADMET and molecular dynamics analyses to evaluate their pharmacokinetic and pharmacodynamic behaviour. These *in silico* studies provide insights into the compounds' activity and interactions within biological systems.

EXPERIMENTAL

The melting points were measured using a Stuart Scientific SMP3 apparatus and are reported uncorrected. Infrared spectra were obtained on a BOMEM MB-Series instrument. Proton (300 MHz) and carbon (75 MHz) NMR spectra were recorded on a Bruker AC-300 spectrometer, with chemical shifts referenced to internal TMS. Electron-impact mass spectra were measured on a Micromass GCT system. Elemental compositions were determined using a Perkin-Elmer CHN 2400 analyzer. Thin-layer chromatography was carried out on Merck silica gel 60 F_{254} plates supported on aluminium sheets, while column chromatography was performed using silica gel as the stationary phase.

Synthesis of 2-mercaptobenzimidazole derivatives (3a-l): A series of benzimidazole derivatives were synthesized using *o*-phenylenediamine (0.04 mol) and either *N*-aminorhodanine (0.04 mol) or rhodamine (0.04 mol) as starting materials. The reaction mixture was refluxed in xylene for 8 h. The resulting solids were filtered and purified by recrystallization from ethanol (**Scheme-I**).

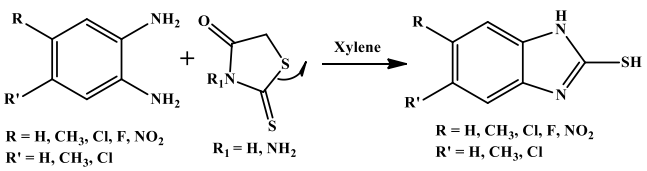

Scheme-I: Synthesis of 2-mercaptobenzimidazoles

Benzimidazole-2-thione (3a): Yield: 90%, m.p.: 200 ºC; FTIR (KBr, ν_{max}, cm^{-1}): 3110.6 (C–H), 2552 (SH), 1496 (C=C); ^{1}H NMR (DMSO-d_6, δ ppm): 7.10 (m, 2H arom.), 7.27 (m, 2H arom.), 12.35 (s, NH); ^{13}C NMR (DMSO-d_6, δ ppm): 120.60 (CH); 126.32 (CH); 138.81 (C), 167.16 (C=S); HRMS *m/z* (found): 150.0251.

5(6)-Nitrobenzimidazole-2-thione (3b): Yield: 81%; m.p.: 210 ºC; ^{1}H NMR (DMSO-d_6, δ ppm): 7.12 (d, J_{AB} = 8.3 Hz, 1H arom); 7.29 (q, J_{BX} = 2.1 Hz, J_{AB} = 8.3 Hz, 1H arom.); 7.46 (d, J_{BX} = 2.1 Hz, 1H arom.), 12.03 (s, NH); ^{13}C NMR (DMSO-d_6, δ ppm): 108.24 (CH); 113.46 (CH); 125.70 (CH); 137.45 (C); 141.94 (C); 148.01 (C); 167.54 (C=S); HRMS *m/z* (found): 195.03157.

5(6)-Methylbenzimidazole-2-thione (3c): Yield: 85%, m.p.: 290 ºC, ^{1}H NMR (DMSO-d_6, δ ppm): 2.21 (s, CH_3), 6.43 (d, J_{AB} = 8.3 Hz, 1H arom.); 6.83 (q, J_{BX} = 1.7 Hz, J_{AB} = 8.3 Hz, 1H arom.); 7.05 (d, J_{BX} = 1.7 Hz, 1H arom.); 11.59 (s, NH); ^{13}H NMR (DMSO-d_6, δ ppm): 109.50 (CH), 109.99 (CH), 123.49 (CH), 130.69 (C), 131.92 (C), 132.95 (C), 168.12 (C=S); HRMS *m/z* (found): 164.01257.

5(6)-Chlorobenzimidazole-2-thione (3d): Yield: 79%, colour: brown, m.p.: 233 ºC; FTIR (KBr, ν_{max}, cm^{-1}): 3111 (C–H arom.), 2553 (S–H), 1510.65 (C=C), 1612.3 (C=N). ^{1}H NMR (DMSO-d_6, δ ppm): 6.81 (d, J_{AB} = 7.9 Hz, 1H arom), 7.03 (q, J_{BX} = 1.9 Hz, J_{AB} = 7.9 Hz, 1H arom), 7.25 (d, J_{BX} = 1.9 Hz, 1H arom), 11.83 (s, NH); ^{13}C NMR (DMSO-d_6, δ ppm): 101.34 (CH); 109.64 (CH); 123.71 (CH); 135.54 (C); 140.84 (C); 146.14 (C); 165.24 (C=S). HRMS, HRMS *m/z* (found): 183.9992.

5,6-Dichloro-1*H*-benzoimidazole-2-thione (3e): Yield: 75%, colour: white, m.p.: 218 ºC; ^{1}H NMR (DMSO-d_6, δ ppm): 7.79 (s, 1H arom.); 11.82 (s, NH); ^{13}C NMR (DMSO-d_6, δ ppm): 101.34 (CH); 109.64 (CH); 123.71 (CH); 135.54 (C); 140.84 (C); 146.14 (C); 168.24 (C=S); HRMS *m/z* (found): 217.0125.

5,6-Dimethylbenzimidazole-2-thione (3f): Yield: 80%; colour: brown, m.p.: 215 ºC; FTIR (KBr, ν_{max}, cm^{-1}): 3111 (C–H arom.); 2553 (S–H); 1510.65 (C=C); 1612.3 (C=N); ^{1}H NMR (DMSO-d_6, δ ppm): 2.32 (s, CH_3); 7.02 (s, 1H arom.); 12.63 (s, NH); ^{13}C NMR (DMSO-d_6, δ ppm): 20.43 (CH_3); 109.50 (CH); 110.99 (CH); 131.19 (CH); 131.69 (C); 168 (C=S); HRMS *m/z* (found): 1780.0214.

5(6)-Flourbenzimidazole-2-thione (3h): Yield: 79%, colour: white, m.p.: 129 ºC, FTIR (KBr, ν_{max}, cm^{-1}): 3111 (C–H arom.), 2553 (S–H); 1510.65 (C=C); 1612.3 (C=N); ^{1}H NMR (DMSO-d_6, δ ppm): 6.85 (d, J_{AB} = 7.92 Hz, 1H arom.); 7.08 (d, J_{BX} = 1.9 Hz, J_{AB} = 7.9 Hz, ^{1}H arom.); 7.26 (d, J_{BX} = 1.9 Hz, 1H arom); 11.88 (s, NH); ^{13}C NMR (DMSO-d_6, δ ppm): 101.38 (CH); 109.66 (CH); 123.74 (CH); 135.54 (C); 140.84 (C); 146.14 (C); 166.24 (C=S); HRMS *m/z* (found): 168.196.

Benzimidazole-2-thione-carboxylic acid (3l): Yield: 41%, colour: white, m.p: 280 ºC; FTIR (KBr, ν_{max}, cm^{-1}): 3111 (C–H arom.), 2553 (S–H), 1510.6 (C=C), 1612.3 (C=N), 1672 (C=O); ^{1}H NMR (DMSO-d_6, δ ppm): 6.85 (d, J_{AB} = 7.92 Hz, 1H arom.); 7.08 (q, J_{BX} = 1.9 Hz, J_{AB} = 7.9 Hz, 1H arom.); 7.26 (d, J_{BX} = 1.9 Hz, 1H ar); 11.88 (s, NH); ^{13}C NMR

(DMSO-d_6, δ ppm): 101.38 (CH); 109.66 (CH); 123.74 (CH); 135.54 (C); 140.84 (C); 146.14 (C); 166.24 (C=S); 176 (COOH); HRMS *m/z* (found): 194.0235.

Synthesis of 2-mercaptobenzoxazole derivatives (4a-c): 2-Mercaptobenzoxazole derivatives were synthesized using *o*-aminophenol with either *N*-aminorhodanine or rhodamine under the same reaction conditions as above (**Scheme-II**). The reaction mixture was refluxed in xylene for 8 h. The resulting solids were filtered and purified by recrystallization from ethanol.

Benzoxazole-2-thione (4a): Yield: 92%; colour: white; m.p.: 198 ºC; FTIR (KBr, ν_{max}, cm^{-1}): 3110.6 (C–H), 2552 (SH), 1595 (C=N), 1496 (C=C); ^{1}H NMR (DMSO-d_6, δ ppm): 6.90 (m, 2H arom.), 7.3 (m, 2H arom.), 7.37 (m, 2H arom.), 7.57 (m, 2H arom.); ^{13}C NMR (DMSO-d_6, δ ppm): 110.6 (C, CH), 111.32 (CH), 122.81 (C), 126.6 (CH), 130.32 (CH), 148.81 (C), 174.16 (C=S); HRMS *m/z* (found): 151.0175.

5(6)-Methylbenzoxazole-2-thiol (4b): Yield: 85%, colour: brown, m.p.: 222 ºC; FTIR (KBr, ν_{max}, cm^{-1}): 3110.6 (C–H), 2552 (SH), 1595 (C=N), 1496 (C=C); ^{1}H NMR (DMSO-d_6, δ ppm): 2.27 (s, CH_3), 6.67 (d, J_{AB} = 8.3 Hz, 1H arom.), 6.86 (q, J_{BX} = 1.7 Hz, J_{AB} = 8.3 Hz, 1H arom.), 7.25 (d, J_{BX} = 1.7 Hz, 1H arom.); ^{13}C NMR (DMSO-d_6, δ ppm): 21.21 (CH_3), 110.50 (CH), 121.99 (CH), 127.49 (CH), 128.69 (C), 134.92 (C), 144.95 (C), 160.12 (C=S); HRMS *m/z* (found): 165.0254.

5(6)-Nitrobenzoxazole-2-thione (4c): Yield: 87%; colour: yellow, m.p.: 230 ºC; IR (KBr, ν_{max}, cm^{-1}): 3051 (C–H arom.); 2550 (S–H), 1607 (C=N), 1506 (NO_2), 1466 (C=C); ^{1}H NMR (DMSO-d_6, δ ppm): 7.5 (d, J_{AB} = 8.3 Hz, 1H arom.); 8.3 (d, J_{BX} = 2.1 Hz, J_{AB} = 8.3 Hz, 1H arom.), 8.4 (s, J_{BX} = 2.1 Hz, 1H arom.); ^{13}C NMR (DMSO-d_6, δ ppm): 109.24 (CH); 115.46 (CH); 120.70 (CH); 137.45 (C); 144.94 (C); 148.99 (C); 182.54 (C=S); HRMS *m/z* (found): 196.0202.

Synthesis of 2-mercaptobenzothiazole derivative (5a): Similarly, 2-mercaptobenzothiazole derivative was synthesized from *o*-aminothiophenol (0.04 mol) and either *N*-aminorhodanine or rhodamine (0.04 mol) under the same reaction conditions as above (**Scheme-II**). The reaction mixture was refluxed in xylene for 8 h. The resulting solids were filtered and purified by recrystallization from ethanol.

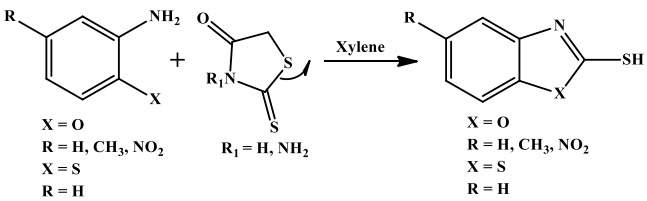

Scheme-II: Synthesis of 2-mercaptobenzoxazoles and 2-mercaptobenzothiazoles derivatives [Ref. 12]

Benzothiazole-2-thiol (5a): Yield: 92%, colour: white, m.p.: 198 ºC; IR (KBr, ν_{max}, cm^{-1}): 3099 (C–H arom.), 2530 (S–H), 1604.15 (C=N); ^{1}H NMR (DMSO-d_6, δ ppm): 7.92 (m, 2H arom), 8.36 (m, 2H arom), 8.40 (m, 2H arom), 8.6 (m, 2H arom); ^{13}C NMR (DMSO-d_6, δ ppm): 120.6 (C, CH), 121.32 (CH), 128.81 (C), 130.6 (C, CH), 140.32 (CH), 145.81 (C), 177.16 (C=S); HRMS *m/z* (found): 167.0241.

Docking, ADMET and molecular dynamics: The computational studies were conducted to evaluate the interactions, pharmacokinetics and dynamic behaviour of the synthesized compounds. Molecular docking was performed to predict the ligand-receptor interactions, involving sampling to generate potential binding positions and scoring to evaluate binding strength. Docking studies utilized Schrödinger Maestro 13.4 software with Glide HTVS, SP and XP modules, including LigPrep, PrepWizard, grid generation and docking calculations [34]. Target protein structures related to HIV were obtained from the Protein Data Bank (PDB) and prepared using the Protein Preparation Wizard, including addition of polar hydrogens, removal of water molecules and ions, assignment of bond orders and charge definition at pH 7.0. Grid boxes were centered on co-crystallized ligands, and ligands were docked using SP, XP and HTVS algorithms to identify optimal binding conformations.

ADMET properties (absorption, distribution, metabolism, excretion, and toxicity) of the benzimidazole-2-thione, benzoxazole-2-thione and benzothiazole-2-thione derivatives were predicted using the PreADMET predictor. To validate docking results and assess binding stability, molecular dynamics (MD) simulations of the ligand-receptor complexes were performed using GROMACS. The simulation protocol included energy minimization, equilibration and production run under physiologically relevant conditions, with a total simulation time of 100 ns. Trajectories were analyzed to evaluate root-mean-square deviation (RMSD), root-mean-square fluctuation (RMSF) and radius of gyration (Rg) using the gmx rms, gmx rmsf and gmx gyrate functions [34-40].

HSV and HIV docking studies: Molecular docking to evaluate the potential activity of the synthesized compounds against HIV and HSV targets was performed [41] to predict ligand binding modes and affinities. The ligands were prepared using the LigPrep wizard in Maestro 13.4 [37], where structures were converted to 3D, hydrogen atoms were added, bond lengths and angles were optimized and energy minimization was performed using the OPLS4 force field. Chirality was preserved and ionization states were kept as default. The starting geometries of the target proteins were obtained from the RCSB Protein Data Bank: HIV-1 protease (PDB ID: 5CON) and unliganded HSV Gd (PDB ID: 2C3A). Target selection was based on protein function, high-quality structural resolution and well-defined binding sites suitable for docking. Proteins were prepared using Maestro 13.4 Protein Preparation Wizard, including preprocessing, refinement and structural optimization. Potential binding sites were identified and analyzed using SiteMap, considering protein size, functionality, solvent exposure and site scores to rank their suitability for ligand binding. Receptor grids were generated at the identified active sites, and ligands were docked using Glide with three precision modes: HTVS (high-throughput virtual screening), SP (standard precision) and XP (extra precision). Docking evaluated ligand-protein interactions, including binding energies (kcal/mol), internal energy, RMSD, desolvation energy, hydrogen bonding, lipophilic contacts and π-stacking interactions.

RESULTS AND DISCUSSION

In this work, novel derivatives of 2-mercaptobenzimidazole, 2-mercaptobenzoxazole and 2-mercaptobenzothiazole

were synthesized through condensation of *o*-phenylenediamine, *o*-aminothiophenol or *o*-aminophenol with rhodanine or N-aminorhodanine. The structural characterization was achieved *via* ^{1}H & ^{13}C NMR, FTIR and HRMS techniques. For benzimidazole-2-thione derivatives, melting points were approximately 250 ºC. Compound **3a** displayed the highest yield of 90%, while compounds **3b**, **3c** and **3f** were obtained in 81%, 85% and 80% yields, respectively. In comparison, benzoxazole-2-thione and benzothiazole-2-thione derivatives showing melting points around 200 ºC. Notably, compounds **4a** and **5a** showed yields of 82% and 90%, respectively, highlighting the efficiency of the synthetic protocol. The ^{1}H NMR spectra confirmed the presence of the N–H proton, while the ^{13}C NMR spectra showed the characteristic C=S signal, verifying the formation of thione derivatives. FTIR spectra further supported the structural assignment. Overall, the spectral and analytical data consistently confirmed the successful synthesis of the target derivatives, with yields and physical properties correlating well across the three heterocyclic scaffolds.

Docking studies: The molecular docking scores of the synthesized molecules **3a-l**, **4a-c** and **5a** and the amino acids found in the active sites of 5CON and 2C3A are showed in Table-1. Proteins targets have the hydrogen bond attractors and hydrogen bond donors with the amino acids in the binding site. The 2D structures of the most active compounds interacting with the amino acids in the binding site of the 5CON and 2C3A are also mapped in Table-2.

TABLE-1
PREDICTION OF BINDING ENERGIES OF
5CON AND 2C3A WITH COMPOUNDS **3a-l, 4a-c** AND **5a**

Compounds	5CON			2C3A		
	HTVS	SP	XP	HTVS	SP	XP
3a	-5.2	-5.6	-3.6	-4.2	-5.6	-3.8
3b	-5.1	-5.8	-3.8	-4.6	-5.6	-4.0
3c	-5.3	-5.4	-3.8	-6.0	-6.8	-5.0
3d	-5.2	-5.8	-4.0	-5.2	-5.6	-4.0
3e	-5.0	-5.5	-4.1	-5.0	-5.3	-4.0
3f	-5.2	-5.6	-3.8	-4.4	-6.8	-5.0
3g	-5.4	-5.8	-4.0	-6.0	-5.7	-4.7
3h	-5.3	-5.9	-4.2	-6.1	-6.7	-4.8
3i	-5.7	-6.5	-4.3	-5.7	-7.0	-4.8
3j	-5.4	-5.0	-3.8	-6.4	-6.8	-5.0
3k	-5.1	-5.6	-4.0	-4.4	-6.8	-5.0
3l	-6.3	-6.3	-4.2	-6.1	-6.5	-4.6
4a	-5.5	-6.1	-6.7	-5.0	-5.8	-5.5
4b	-5.8	-6.3	-6.7	-5.3	-7.0	-7.1
4c	-6.0	-6.1	-6.1	-5.5	-6.3	-6.4
5a	-5.3	-5.5	-5.5	-3.8	-3.8	-3.8
Abacavir	-5.7	-6.2	-5.1	-3.5	-3.9	-4.5

The binding energies of the studied complexes range is varying from -3.6 to -6.7 kcal/mol for complexes 5CON-(**3a-l**, **4a-c** and **5a**) and from -3.8 to -7.1 kcal/mol for complexes 2C3A-(**3a-l**, **4a-c** and **5a**). Based on the molecular docking results, compound **4b** exhibited the high affinity for the targeted HIV and HSV proteins in the different docking modes. The binding energies were -6.7 kcal/mol for 5CON and -7.1 kcal/mol for 2C3A in extra precision (XP) mode, -6.3 kcal/mol and -7.0 kcal/mol in standard precision mode and -5.8 kcal/mol and -5.3 kcal/mol in HTVS precision mode, respectively. The interactions are detailed in Table-2. To evaluate the efficacy of the binding for compound **4b**, a reference drug abacavir was also computed for docking. Abacavir showed a binding energy of -6.2 kcal/mol which is comparable to the results obtained for compound **4b**. These findings suggest that **4b** have the potential to serve as promising inhibitors of HSV and HIV viruses. A comprehensive analysis was conducted for this molecule to well understand the involved interactions and their contribution in the stability of complex (Table-2).

Toxicity, ADME and drug likeness: After the docking study, compound **4b** was identified as having the highest antiviral activity. Consequently, toxicity, ADME and drug-likeness assessments were conducted for compound **4b** and abacavir (reference drug) using the PreADMET server [38] to evaluate their suitability for pharmaceutical development. The results are summarized in Table-3.

Drug-likeness predictions, based on Lipinski's rule of five and the lead-like rule, were performed using PreADMET's module. ADME predictions employed *in vitro* models, including CaCo2 and MDCK cells, and *in silico* models for human intestinal absorption (HIA) and skin permeability. Toxicity predictions utilized validated models such as the AMES test and rodent carcinogenicity assays.

The drug-likeness results classified both compound **4b** and abacavir as mid-structure, indicating moderate structural complexity associated with a balance between efficacy, bioavailability and ease of synthesis. In terms of MDDR-like rule violations, compound **4b** exhibited violations in no rings and no rotatable bonds, suggesting a lack of aromatic rings and rotatable bonds, which may affect flexibility and binding. Abacavir had a single violation in no rotatable bonds, indicating potential for consistent target binding. Overall, compound **4b** had two MDDR like rule violations, while abacavir had one, remaining closer to conventional drug-like profiles. Both compounds were classified as suitable under Lipinski's rule of five, showing zero violations and suggesting good oral bioavailability. These findings indicate that both compound **4b** and abacavir possess promising drug-like characteristics, with compound **4b** demonstrating a balance between activity, specificity and pharmacokinetics comparable to abacavir.

Toxicity assessment revealed that both compound **4b** and abacavir displayed carcinogenic potential in mouse models, as indicated by positive results in the carcino mouse test. However, the mutagenicity profiles differed, for example, compound **4b** showed mutagenicity in TA100_10RLI and TA100_NA tests but was negative in TA1535_NA, while abacavir showed the opposite trend. Moreover, both compounds exhibited mutagenicity in the TA1535_10RLI test with 10% rat liver extract. These results highlight potential toxicological risks relevant for clinical evaluation.

ADME analysis demonstrated distinct pharmacokinetic properties. Compound **4b** showed moderate blood-brain barrier permeability and acted as a CYP2C19 inhibitor, whereas abacavir displayed low BBB permeability and no CYP2C19 inhibition. Both compounds had high intestinal absorption,

TABLE-2
DOCKING RESULTS AND INTERACTIONS FOR COMPOUND **4b** AND ABACAVIR

Complex	2D diagram	İnteractions
Protein (5CON) – Compound **4b**		
By HTVS precision mode	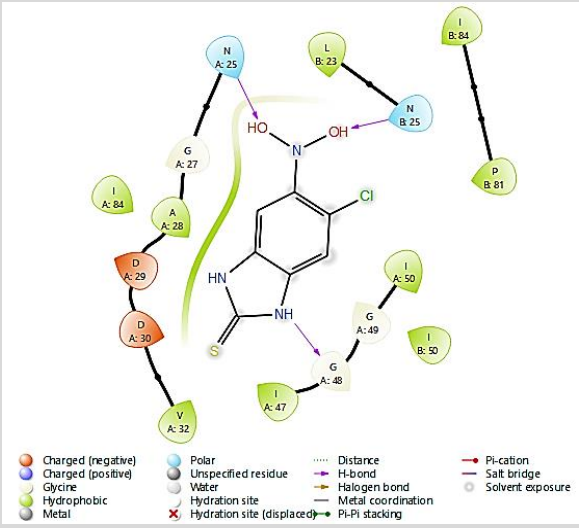	**Affinity score:** -5.8 Kcal/mol **Intercations:** H-bond (N B:25, G A:48)
By standard precision mode	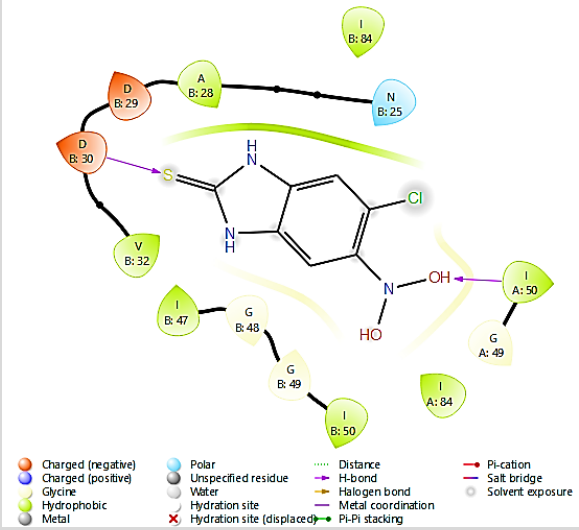	**Affinity score:** -6.3 kcal/mol **Intercations:** H-bond (IA:50, DB:30)
By extra precision mode	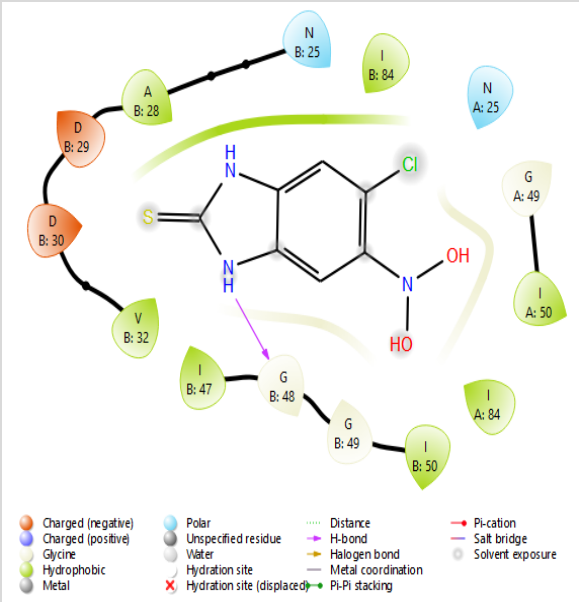	**Affinity score:** -6.7 kcal/mol **Intercations:** H-bond (GB:48)

Protein (2C3A) – Compound (**4b**)		
By HTVS precision mode	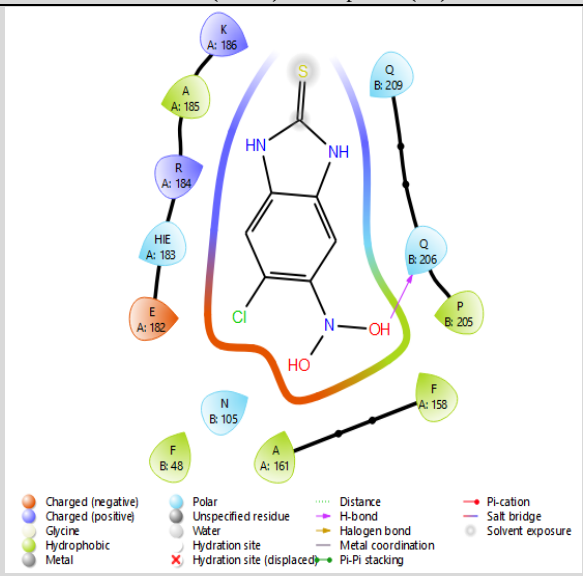	**Affinity score:** -5.3 kcal/mol **Intercations:** H-bond (QB:206)
By standard precision mode	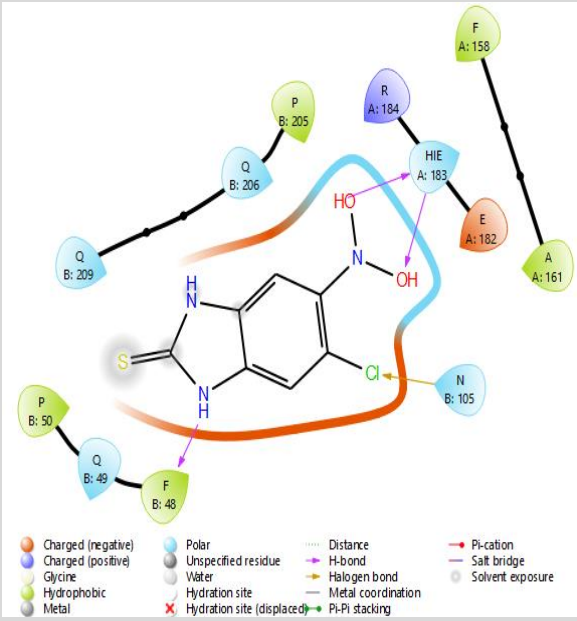	**Affinity score:** -7.0 kcal/mol **Intercations:** H-bond (2 x HIE A:183, F B:48), Halogen bond Cl (N B:105)
By extra precision mode	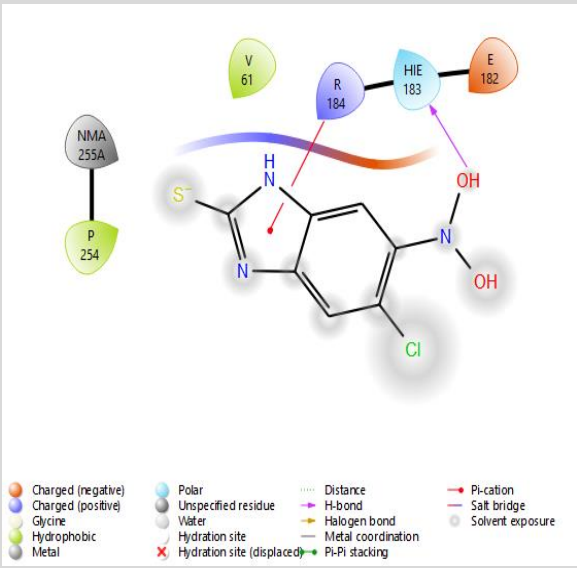	**Affinity score:** -7.1 kcal/mol **Intercations:** H-bond (HIE 183), Pi-cation (R 184)

Protein (2C3A) – Abacavir		
By standard precision	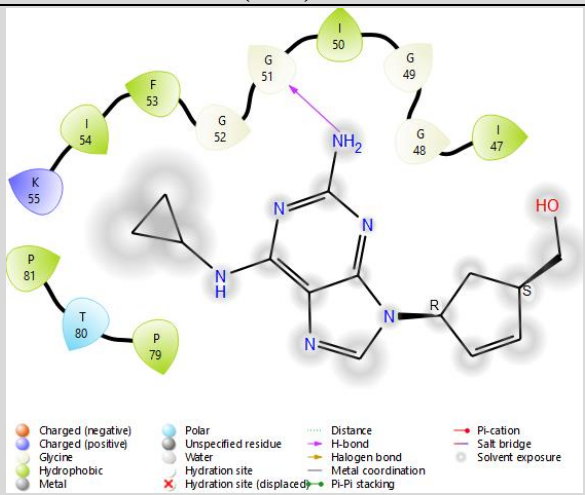	**Affinity score:** -6.2 kcal/mol **Intercations:** H-bond (G 51)

TABLE-3
ADME, TOXICITY AND DRUG LIKENESS FOR COMPOUND **4b** AND ABACAVIR

Study	ID	Values	
		Compound **4b**	Abacavir
Druglikeness	MDDR like rule	Mid-structure	Mid-structure
	MDDR like rule violation fields	No rings, no rotatable bonds	No rotatable bonds
	MDDR like rule violations	2	1
	Rule of five	Suitable	Suitable
	Rule of five violations	0	0
Toxicity	Carcino mouse	Positive	Positive
	TA100 10RLI	Positive	Negative
	TA100 NA	Positive	Negative
	TA1535 10RLI	Positive	Positive
	TA1535 NA	Negative	Positive
ADME	BBB	2,05654	0.0640829
	CYP 2C19 inhibition	Inhibitor	Non
	HIA	98,137593	89,963215
	MDCK	77,5994	2,87731
	Plasma protein binding	75,603691	47,968425
	Pure water solubility (mg L)	20,4567	255,933

with **4b** slightly higher (98.13%). Compound **4b** exhibited moderate MDCK permeability, high plasma protein binding, and moderate water solubility, whereas abacavir showed lower MDCK permeability, moderate plasma protein binding and high water solubility. These profiles suggest compound **4b** may influence drug metabolism and CNS exposure, while abacavir maintains conventional pharmacokinetic behavior.

Molecular dynamics simulations of the **4b** –protein 2C3A complex were conducted using GROMACS 2023 for 100 ns, employing the GROMOS96 43a1 force field [42]. The system was prepared using pdb2gmx and ligand topologies generated *via* ProdDrug, solvated in a cubic box with 0.15 M NaCl and energy-minimized. Temperature and pressure were maintained at 315 K and 1 bar, respectively. RMSD analysis (Fig. 1) showed rapid adjustment during the first 10 ns, followed by stabilization around 0.6 nm, indicating a stable ligand-protein conformation. RMSF analysis (Fig. 2) revealed higher flexibility in the first 1000 residues (up to 0.3 nm), with the rest of the protein remaining stable (0.1-0.2 nm). The radius of gyration (Rg) remained stable between 3.88–3.90 nm over

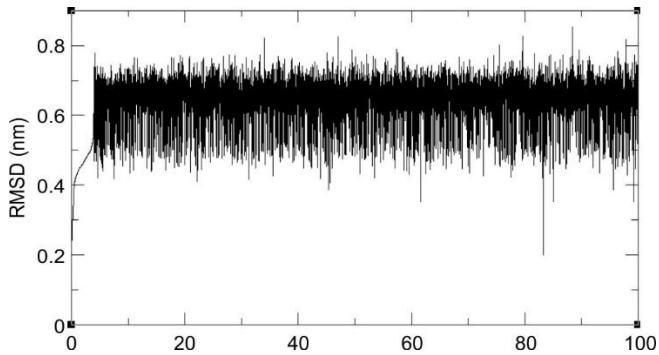

Fig. 1. RMSD Values for complex compound **4b** protein 2C3A

100 ns (Fig. 3), indicating consistent structural compactness. Hydrogen bond analysis (Fig. 4) showed dynamic interactions fluctuating between 0-2 bonds, reflecting the moderate stability of the ligand-protein interaction. Overall, molecular dynamics results confirm that the **4b**–2C3A complex maintains structural stability and moderate flexibility, supporting its potential as a viable antiviral candidate.

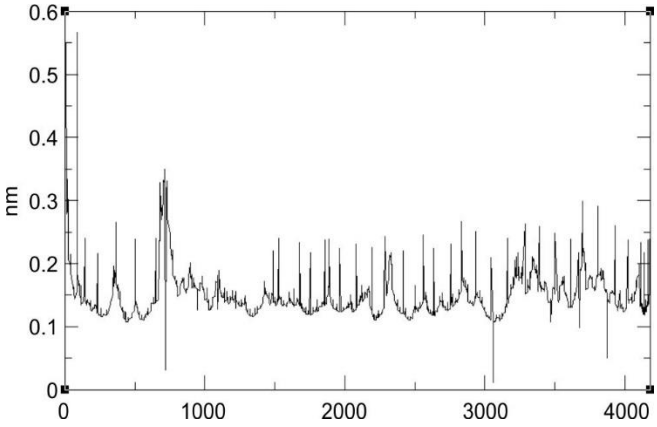

Fig. 2. RMSF values for complex compound **4b** protein 2C3A

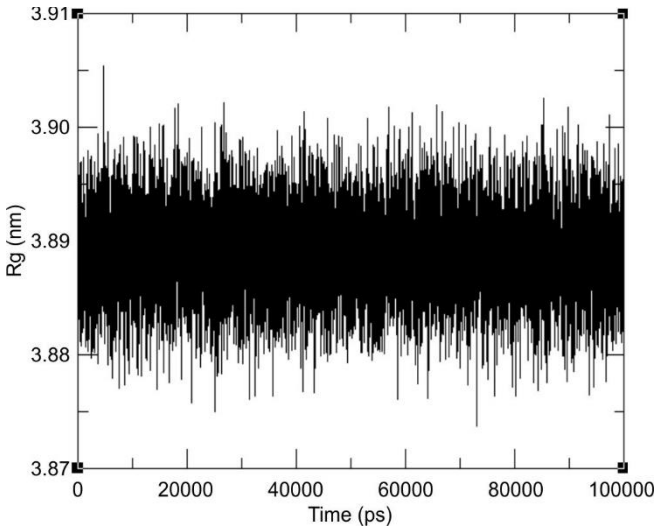

Fig. 3. Rg values for complex compound **4b** protein 2C3A

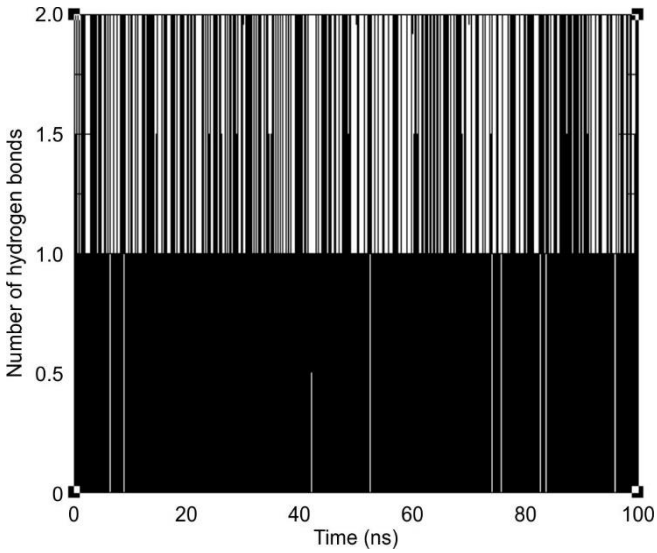

Fig. 4. Hydrogen bonds for complex compound **4b** protein 2C3A

Conclusion

In this study, we successfully developed efficient synthetic methodologies for derivatives of 2-mercaptobenzimidazole, 2-mercaptobenzoxazole and 2-mercaptobenzothiazole *via* condensation of *o*-phenylenediamine, *o*-aminothiolphenyl, and o-aminophenol, respectively with N-aminorhodanine or rhodanine. All the synthesized compounds were characterized using NMR, FTIR, and HRMS, and exhibited satisfactory yields ranging from 70% to 90%. Among the synthesized derivatives, compound **4b** emerged as a particularly promising candidate for antiviral activity against HIV and HSV. Molecular docking studies demonstrated that compound **4b** exhibits strong binding affinity to the target proteins 5CON and 2C3A, with binding energies of -6.7 and -7.1 kcal/mol, respectively, comparable to the reference drug abacavir. The toxicity and ADME evaluations indicated favourable oral bioavailability, drug-likeness and acceptable pharmacokinetic properties, with profiles suggesting a balance between potency and safety, despite some structural liabilities. Molecular dynamics simulations over a 100 ns trajectory revealed that compound **4b** forms a stable complex with protein 2C3A, maintaining structural integrity as evidenced by RMSD, RMSF and Rg analyses. Persistent hydrogen bonding interactions further confirmed the moderate stability of the ligand-protein complex. Thus based on the integrated computational and experimental analyses, compound **4b** possesses significant potential as an antiviral agent. Its strong binding affinity, favourable pharmacokinetic properties and structural stability highlight **4b** as a promising lead for further development and optimization in the pursuit of novel therapeutics against HIV and HSV infections.

CONFLICT OF INTEREST

The authors declare that there is no conflict of interests regarding the publication of this article.

REFERENCES

1. E.R. El-Sawy, A.B. Abdelwahab and G. Kirsch, *Molecules*, **27**, 2150 (2022); https://doi.org/10.3390/molecules27072150
2. T. Kosmalski, R. Kołodziejska, M. Przybysz, Ł. Szeleszczuk, H. Pawluk, K. Mądra-Gackowska and R. Studzińska, *Int. J. Mol. Sci.*, **25**, 9474 (2024); https://doi.org/10.3390/ijms25179474
3. M.T. Chhabria, S. Patel, P. Modi and P.S. Brahmkshatriya, *Curr. Top. Med. Chem.*, **16**, 2841 (2016); https://doi.org/10.2174/1568026616666160506130731
4. M. Conda-Sheridan and M. Krishnaiah, *Methods Mol. Biol.*, **2103**, 111 (2020); https://doi.org/10.1007/978-1-0716-0227-0_7
5. R.J. Spears, C. McMahona and V. Chudasama, *Chem. Soc. Rev.*, **50**, 11098 (2021); https://doi.org/10.1039/D1CS00271F
6. A. Das, M.W. Ashraf and B.K. Banik, *ChemistrySelect*, **6**, 9069 (2021); https://doi.org/10.1002/slct.202102398
7. R.S. Keri, M.R. Patil, S.A. Patil and S. Budagumpi, *Eur. J. Med. Chem.*, **89**, 207 (20215); https://doi.org/10.1016/j.ejmech.2014.10.059
8. H.T. Hamad, *MedMat*, **2**, 17 (2025); https://doi.org/10.1097/mm9.0000000000000012
9. E. Şener, İ. Yalçin and E. Sungur, *Act. Relat.*, **10**, 223 (1991); https://doi.org/10.1002/qsar.19910100308
10. L.L. Bozec and C.J. Moody, *Aust. J. Chem.*, **62**, 639 (2009); https://doi.org/10.1071/CH09126
11. P.C. Sharma, A. Sinhmar, A. Sharma, H. Rajak and D.P. Pathak, *J. Enzyme Inhib. Med. Chem.*, **28**, 240 (2013); https://doi.org/10.3109/14756366.2012.720572

12. A. El Kihel, H. Sir, S. Jebbari, M. Ahbala, S. Guesmi and P. Bauchat, *Orient. J. Chem.*, **32**, 1765 (2016); https://doi.org/10.13005/ojc/320405
13. A. Irfan, F. Batool, S.A. Zahra Naqvi, A. Islam, S.M. Osman, A. Nocentini, S.A. Alissa and C.T. Supuran, *J. Enzyme Inhib. Med. Chem.*, **35**, 265 (2020); https://doi.org/10.1080/14756366.2019.1698036
14. M.A. Morsy, E.M. Ali, M. Kandeel, K.N. Venugopala, A.B. Nair, K. Greish and M. El-Daly, *Antibiotics*, **9**, 221 (2020); https://doi.org/10.3390/antibiotics9050221
15. G.L. Khatik, A.K. Datusalia, W. Ahsan, P. Kaur, M. Vyas, A. Mittal and S.K. Nayak, *Curr. Drug Discov. Technol.*, **15**, 163 (2018); https://doi.org/10.2174/1570163814666170915134018
16. S. Shafi, M. Mahboob Alam, N. Mulakayala, C. Mulakayala, G. Vanaja, A.M. Kalle, R. Pallu and M.S. Alam, *Eur. J. Med. Chem.*, **49**, 324 (2012); https://doi.org/10.1016/j.ejmech.2012.01.032
17. N. Siddiqui, S.N. Pandeya, S.A. Khan, J. Stables, A. Rana, M. Alam, M.F. Arshad and M.A. Bhat, *Bioorg. Med. Chem. Lett.*, **17**, 255 (2007); https://doi.org/10.1016/j.bmcl.2006.09.053
18. K. Bhagdev and S. Sarkar, *Med. Sci. Forum*, **7**, 9 (2021); https://doi.org/10.3390/ECMS2021-10839
19. H. Gurer-Orhan, C. Karaaslan, S. Ozcan, O. Firuzi, M. Tavakkoli, L. Saso and S. Suzen, *Bioorg. Med. Chem.*, **24**, 1658 (2016); https://doi.org/10.1016/j.bmc.2016.02.039
20. V.N. Telvekar, V.K. Bairwa, K. Satardekar and A. Bellubi, *Bioorg. Med. Chem. Lett.*, **22**, 649 (2012); https://doi.org/10.1016/j.bmcl.2011.10.064
21. S. Sarkar, A.A. Siddiqui, S.J. Saha, R. De, S. Mazumder, C. Banerjee, M.S. Iqbal, S. Nag, S. Adhikari and U. Bandyopadhyay, *Antimicrob. Agents Chemother.*, **60**, 4217 (2016); https://doi.org/10.1128/AAC.01575-15
22. J.A. Cairns, *Pulm. Pharmacol. Ther.*, **18**, 55 (2005); https://doi.org/10.1016/j.pupt.2004.09.032
23. Z.A. Bhavsar, P.T. Acharya, D.J. Jethava and H.D. Patel, *Synth. Commun.*, **50**, 917 (2020); https://doi.org/10.1080/00397911.2019.1695276
24. A. Turksoy, D. Yildiz and E.U. Akkaya, *Coord. Chem. Rev.*, **379**, 47 (2019); https://doi.org/10.1016/j.ccr.2017.09.029
25. D. Kemisetti, R. Amin, F. Alam, A. Gacem, T.B. Emran, T. Alsufyani, M.S. Alqahtani, S. Islam, M.M. Matin and M. Jameel, *Evid. Based Complement. Alternat. Med.*, **2023**, e5460563 (2023); https://doi.org/10.1155/2023/5460563
26. C.T. Supuran, *Expert Rev. Neurother.*, **16**, 961 (2016); https://doi.org/10.1080/14737175.2016.1193009
27. El kihel, H. AitSir, S. Jebbari, M. Ahbala, S. Guesmi and P. Bauchat, *Oriental J. Chem.*, **32**, 1765 (2016).
28. M.H. Aboutaleb, N.S. El-Gohary, H.A. Ghabbour and M.M. El-Kerdawy, *Arch. Pharm.*, **356**, 2300269 (2023); https://doi.org/10.1002/ardp.202300269
29. J. Valdez, R. Cedillo, A. Hernández-Campos, L. Yépez, F. Hernández-Luis, G. Navarrete Vázquez, A. Tapia, R. Cortés, M. Hernández and R. Castillo, *Bioorg. Med. Chem. Lett.*, **12**, 2221 (2002); https://doi.org/10.1016/S0960-894X(02)00346-3
30. M. Kidwai, S. Saxena and R. Mohan, *J. Korean Chem. Soc.*, **49**, 288 (2005); https://doi.org/10.5012/jkcs.2005.49.3.288
31. M.-L. Wang and B.-L. Liu, *J. Chin. Inst. Chem. Eng.*, **38**, 161 (2007); https://doi.org/10.1016/j.jcice.2007.01.003
32. R.O. Beauchamp, J.S. Bus, J.A. Popp, C.J. Boreiko, L. Goldberg and M.J. McKenna, *CRC Crit. Rev. Toxicol.*, **11**, 169 (1983); https://doi.org/10.3109/10408448309128255
33. E.C. Vigliani, *Br. J. Ind. Med.*, **11**, 235 (1954); https://doi.org/10.1136/oem.11.4.235
34. K. Sankar, K. Trainor, L.L. Blazer, J.J. Adams, S.S. Sidhu, T. Day, E. Meiering and J.K.X. Maier, *Mol. Inform.*, **41**, 2100240 (2022); https://doi.org/10.1002/minf.202100240
35. R.A. Friesner, R.B. Murphy, M. P. Repasky, J.R. Greenwood, L.L. Frye, T.A. Halgren, P.C. Sanschagrin and D.T. Mainz, *J. Med. Chem.*, **49**, 6177 (2006); https://doi.org/10.1021/jm051256o
36. T.A. Halgren, R.B. Murphy, R.A. Friesner, H.S. Beard, L.L. Frye, W.T. Pollard and J.L. Banks, *J. Med. Chem.*, **47**, 1750 (2004); https://doi.org/10.1021/jm030644s
37. Schrödinger, LLC, Glide, Schrödinger Release 13.4: Glide, Schrödinger, LLC, New York, NY (2022)
38. PreADMET, Prediction of ADME/Tox, BMDRC, [Online]. Available: https://preadmet.webservice.bmdrc.org/
39. M.J. Abraham, T. Murtola, R. Schulz, S. Páll, J.C. Smith, B. Hess and E. Lindahl, *SoftwareX*, **1-2**, 19 (2015); https://doi.org/10.1016/j.softx.2015.06.001
40. GROMACS User Manual, version 2021, [Online]. Available: https://manual.gromacs.org/2021/manual-2021.pdf
41. D.C. Chan and P.S. Kim, *Cell*, **93**, 681 (1998); https://doi.org/10.1016/S0092-8674(00)81430-0
42. GROMOS96 43a1 force field Accessed: Jun. 30, 2023; [Online]. Available: https://www.ks.uiuc.edu/Training/Tutorials/science/forcefield-tutorial/forcefield-html/node5.html